Few-Mode Fibers: Characterizations and Applications

M. Bigot, M. Bsaibes, Laurent Bigot, Y. Quiquempois, P. Sillard

Few-Mode Fibers: Characterizations and Applications

M. Bigot[(1)], M. Bsaibes[(2)], L. Bigot[(2)], Y. Quiquempois[(2)], P. Sillard[(1)]
[(1)]Prysmian Group, Parc des Industries Artois Flandres, 644 boulevard Est, Billy Berclau, 62092 Haisnes Cedex, France
[(2)]Univ. Lille, CNRS, UMR 8523 - PhLAM - Physique des Lasers, Atomes et Molécules, F-59000 Lille, France
Email address: marianne.bigot@prysmiangroup.com

Abstract: We report design guidelines and modal loss characterizations (light scattering and extra-loss phenomena) of few-mode fibers that allow optimizing their crosstalk, differential mode group delay and differential mode attenuation for practical applications.

1. Introduction

Over the past decade, Mode-Division-Multiplexed (MDM) transmissions exploiting the multiple modes (N=3 to 55 spatial modes) of Few-Mode Fibers (FMFs) have demonstrated their ability to overcome the capacity limits of single-mode systems [1-6]. In the weakly-coupled approach, each (group of) mode can be used as an independent data channel, if modal Crosstalk (XT) is minimized. Conventional signal processing techniques can then be used, i.e. simple 2×2 and 4×4 Multiple-Input Multiple-Output (MIMO) with coherent detection or no MIMO with direct detection. In the full-MIMO approach, all modes are simultaneously detected at reception with complex 2N×2N MIMO to compensate for the XT, which requires to minimize their differential mode group delays (DMGDs).

XT and DMGD, that ultimately limit the reach of MDM transmissions, can be reduced by optimizing index profiles [7-15]. However, the attenuation and the Differential Modal Attenuation (DMA) of FMFs, that also degrade transmission performance in both approaches, have been little studied so far. In recent works, we demonstrated that the highest-order modes are more sensitive to Small Angle Light Scattering effect (SALS) and that the index profile can play a significant role on this effect [10]. We notably quantified the contributions of light scattering phenomena (Rayleigh Scattering (RS) and (SALS)) and their impacts on DMA [16].

In this paper, after discussing fiber design guidelines to minimize the XT or the DMGDs of FMFs, we present modal characterizations of light scattering phenomena performed on 3 different 6-LP-mode (10-spatial-mode) fibers. We show that trapezoidal-index profiles offer a good trade-off between low XT and low DMA. Finally, we report some practical applications using optimized FMFs.

2. Fiber Design Guidelines

2.1. Weakly-coupled FMFs

To minimize the XT, a well-known solution consists of increasing the effective index difference between the modes (Δn_{eff}) [7,11]. For a given number of modes in step-index FMFs, this is done by simultaneously increasing the core index and decreasing the core radius. The drawbacks, however, are higher attenuations and smaller effective areas for all the modes [7].

A depressed-index zone can then be introduced in the center of the step-index core, or a high-index ring can be added, to allow increasing the Min$|\Delta n_{eff}|$ between the LP modes from 0.6-0.9×10^{-3} to 1.5-1.8×10^{-3} without impacting attenuations or effective areas [8,9,12,13]. But despite this increase in Min$|\Delta n_{eff}|$, the XT reduction is moderate (~2dB/km) for FMFs with LP modes ≥4, compared to >10dB/km reduction obtained for 2-LP-mode fibers [11] (see Fig.1). This is because the XT does not come only from the 2 modes with the smallest $|\Delta n_{eff}|$, but also from the other modes. More attention should thus be paid to the influence of mode overlapping and light scattering phenomena.

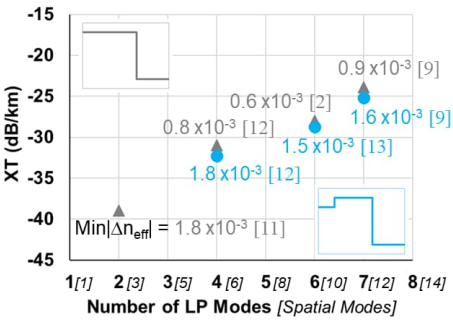

Fig.1: Measured XT vs. number of LP modes for step-index (grey) and inner-depressed step-index (blue) FMFs with different Min$|\Delta n_{eff}|$.

2.2. Low-DMGD FMFs

Trench-assisted graded-index FMFs can guide up to 55 spatial modes with low DMGDs [5]. These FMFs are made with usual multimode processes, allowing for low-cost and large-scale production [14,15]. DMGD is minimized at 1550nm by tuning the alpha parameter that governs the shape of the graded-index core and by taking particular care of the dimension and the position of the trench.

DMGDs are measured at 1550nm with the standard multimode DMGD setup. The different mode groups corresponding to the different peaks of the DMGD plot can be identified by simulating the measured traces using a

convolution of the input pulse and Dirac delta functions centered at the mode-group delays and weighted by the mode power distributions that depend on the offset launch. This allows for accurate characterizations of the FMFs and for fine tuning of the manufacturing processes in order to reach record low DMGDs (less than 80ps/km for a 15-spatial-mode fiber [15]).

3. Characterizations of Light Scattering Phenomena and DMA

In the C-band, the dominant contribution to optical losses is light scattering which is a combination of 2 factors: RS and SALS. RS is a well-known phenomenon that finds its origin in the microscopic heterogeneities of the glass induced by density fluctuations frozen in the glass and by dopant concentrations. It decreases with the order of the mode because higher-order modes are less confined in the doped core, and it decreases with the core index for all the modes. SALS has been less investigated. It is linked to local dipole elements induced by longitudinal and azimuthal fluctuations at the core-cladding interface that causes some coupling with radiation modes [17-19]. It is confined in a small angular cone (<50°) in the propagation direction of the mode. It increases with the order of the mode because higher-order modes have higher amplitude at the core-cladding interface. It also increases as a function of the index gradient at the core-cladding interface.

The relative contributions of each phenomenon in each mode and their impacts on the resulting DMA were quantified on 3 different FMFs designed to guide 6 LP modes (10 spatial modes) with low XT between their (group of) modes [16] (see insets of Fig.2(a)). Modal attenuations were measured at 1550nm by Optical Time Domain Reflectometry (OTDR) combined with a mode multiplexer based on multi-plane light conversion [20] (see Fig.2(a)). Fiber A [9] has an inner-depressed step-index profile and shows a significant increase of attenuation as a function of the mode order (DMA~0.11dB/km). Fiber B [10] has an inner-depressed trapezoidal-index profile (same Min$|\Delta n_{eff}|$ of 1.6×10^{-3}) and presents a much lower DMA of ~0.02dB/km. Such a profile was chosen to reduce SALS while ensuring a sufficiently high Min$|\Delta n_{eff}|$. Fiber C [14] has a trench-assisted graded-index profile, known to minimize SALS [18], with LP modes grouped into mode groups, and has a DMA~0.04dB/km.

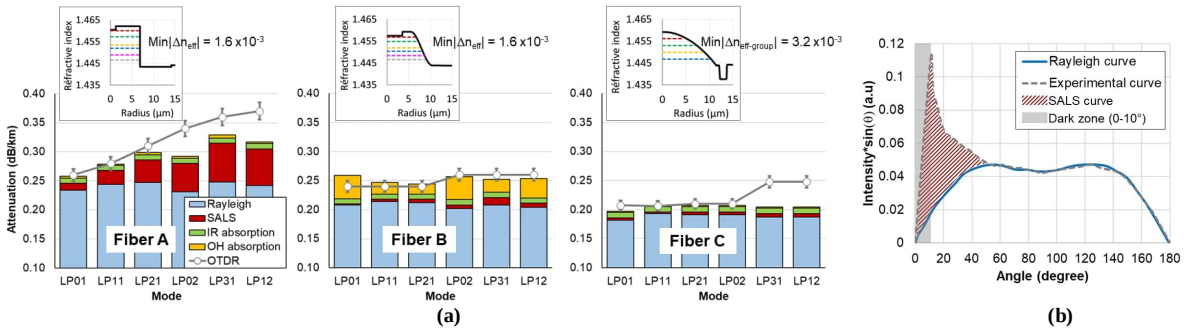

Fig.2: OH, IR, Rayleigh and SALS contributions to the total losses (OTDR) of each mode of the different FMFs with their index profiles at 1550nm in insets (a); Example of experimental angular distribution of scattered intensity measured on Fiber A for LP_{12} mode (dashed line) compared to theoretical Rayleigh curve, both weighted by the solid angle. The excess scattering intensity measured allows extracting the SALS contribution (b).

To quantify SALS and RS contributions, a dedicated light scattering measurement bench was developed [10, 16,17]. It consists of measuring the angular dependence of the normalized scattered light emitted by an uncoated section of the Fiber Under Test (FUT) passing through a circular quartz tank filled with index-matching and coupled to a laser source emitting around 1550nm, successively modulated at low frequency, scrambled in polarization and injected into the input port of the mode multiplexer. The output of the multiplexer is spliced to several meters of the FUT. Taking benefit of the known angular distribution of RS relative to the fiber propagation direction and fitting the data from 50° to 170°, we can extract for each mode the RS contribution. The SALS contribution is extracted by quantifying the excess scattered intensity at small angles (see Fig.2(b)). The RS and SALS contributions were evaluated for the 6 LP modes by measuring each fiber on 5 different longitudinal positions. Fig.2(a) summarizes the results. It can be noticed that Fiber A presents a higher RS contribution (~0.24dB/km) than the two other fibers (~0.21dB/km for Fiber B, and ~0.19dB/km for Fiber C). This is well explained by the core-cladding index difference. As expected, SALS increases with the mode order for Fiber A (from ~0.01dB/km to 0.08dB/km), while the increase is limited for Fiber B (~0.01dB/km) and very low whatever the mode order for Fiber C (<0.01dB/km). This confirms the theory, developed for SMFs [18-19] and highlighted here for FMFs in [10], that SALS contributes significantly to the DMA for the step-index profiles.

The estimated IR and OH absorption contributions have a limited mode order dependency at the scale of total losses. They can be added to the scattering contributions to explain the total losses measured by OTDR, the UV contribution being negligible at 1550nm. It was observed that Fiber B is affected by high OH absorption and that its total losses could be reduced by ~0.02dB/km with a better control of the manufacturing environment. One can note a good agreement between the measured and reconstructed losses. The small differences are attributed to the uncertainties coming from our experimental bench (dark zone below 10°), while the higher difference experienced on the 4th mode group of Fiber C can be explained by micro-bending effects.

4. Applications

In the weakly-coupled approach, using simple 2×2 and 4×4 MIMO, a record capacity of 402.7Tbps was demonstrated over 48km with 10 spatial modes [2] and 525km was reached with 4 spatial modes [3]. Real-time experiments, that lay the ground to actual deployments, were also reported [4,21]. Without MIMO, mode group division multiplexing using direct detection enabled 200Gbps bidirectional transmission over 20 km [1], and the same technique was deployed to multiply the capacity of MMF-based LANs by a factor of 400 [22].

In the full-MIMO approach, MDM with coherent detection allowed demonstrating several records: capacity of 1.53Pbs with spectral efficiency of 332b/s/Hz over 25.9km with 55 spatial modes (110×110 MIMO) [5], and distance of 3250km with 6 spatial modes (12×12 MIMO) [6]. Also, a 15-spatial-mode cable, which is part of the fiber-optic infrastructure of L'Aquila, recently allowed performing in-the-field MDM transmissions [23,24], which will enable a further step toward future deployed transmission systems.

5. Conclusions

XT mechanisms in FMFs are not only a question of mode (group) spacing characterized by $|\Delta n_{eff}|$. Mode overlapping and scattering losses also play an important role. We have shown that trapezoidal-index profiles allow reducing SALS and DMA without degrading mode spacing. Further investigations are still in progress to evaluate the benefit of scattering-loss reductions on XT.

6. Acknowledgments

This work was partially supported by BPI France in the frame of the MODAL project (FUI 19), by ANR in the frame of the MUPHTA project (ANR-20-CE24-0016) and by the Hauts-de-France Regional (HdF) Council, the European Regional Development Fund (ERDF) and the I-SITE UNLE within the eLIFT project.

7. References

[1] K. Benyahya *et al.*, "200Gb/s Transmission over 20km of FMF using Mode Group Multiplexing and Direct Detection," ECOC'18, Tu1G.5.
[2] D. Soma *et al*., "402.7-Tbps Weakly-Coupled 10-Mode Multiplexed Transmission using Rate Adaptive PS PDM-16QAM WDM signals," ECOC'19, W.2.A.2.
[3] M. Zuo *et al.*, "Long-haul intermodal-MIMO-free MDM transmission based on a weakly coupled multiple-ring-core few-mode fiber," Opt. Exp. **30**, 5868–5878 (2022).
[4] Igarashi *et al.*, "Real-time Weakly-coupled Mode Division Multiplexed Transmission over 48 km 10-mode Fibre," ECOC'19, W.2.A.3.
[5] G. Rademacher *et al.*, "1.53 Peta-bit/s C-Band Transmission in a 55-Mode Fiber," ECOC'22, Th3B.2.
[6] K. Shibahara *et al.*, "Long-Haul DMD-Unmanaged 6-Mode-Multiplexed Transmission Employing Cyclic Mode-Group Permutation," OFC'20, Th3H.3.
[7] P. Sillard *et al.*, "Few-Mode Fibers for Mode Division Multiplexed Systems," J. Light. Technol. **32**, 2824–2829 (2014).
[8] R. May and M.N. Zervas, "Few-mode fibers with improved mode spacing," ECOC'15, P.1.13.
[9] M. Bigot-Astruc *et al.*, "Next-Generation Multimode Fibers for Space Division Multiplexing," APC'17 (Networks), NeM3B.4.
[10] M. Bigot *et al.*, "Weakly-Coupled 6-LP-Mode Fiber with Low Differential Mode Attenuation," OFC'19, M1E.3.
[11] R. Maruyama *et al.*, "Relationship Between Mode Coupling and Fiber Characteristics in Few-Mode Fibers Analyzed Using Impulse Response Measurements Technique," J. of Lightw. Technol. **35**, 650–656 (2017).
[12] L. Ma *et al.*, "Ring-assisted 7-LP-mode fiber with ultra-low intermode crosstalk," ACP'16, AS4A.5.
[13] D. Ge *et al.*, "Design of a Weakly-Coupled Ring-Core FMF and Demonstration of 6-mode 10-km IM/DD Transmission," OFC'18, W4K.3.
[14] P. Sillard *et al*, "Micro-Bend-Resistant Low-Differential-Mode-Group-Delay Few-Mode Fibers," J. of Lightw. Technol. **35**, 734–740 (2017).
[15] P. Sillard, "Advances in few-mode fiber design and manufacturing," OFC'20, W1B.4.
[16] M. Bsaibes *et al.*, "Light Scattering Mechanisms in Few-Mode Fibers," J. Light. Technol. **40**, 3293–3298 (2022).
[17] P. Guenot *et al.*, "Influence of drawing temperature on light scattering properties of single-mode fibers," OFC'99, Th2G.1.
[18] M.E. Lines *et al*., "Explanation of anomalous loss in high delta singlemode fibers," Electron. Lett. **35**, p.1009 (1999).
[19] P. Mazumder *et al.*, "Analysis of excess scattering in optical fibers," J. Appl. Phys. **96**, 4042–4049 (2004).
[20] G. Labroille *et al.*, "Efficient and mode selective spatial mode multiplexer based on multi-plane light conversion," Opt. Ex. **22**, 15599–15607 (2014).
[21] D. Ge *et al.*, "Demonstration of Real-time Unrepeatered MDM Transmission over 200-km FMF with Commercial 400G System and ROPA," ECOC'22, Tu5.36.
[22] K. Lengle *et al.*, "4×10 Gbit/s bidirectional transmission over 2 km of conventional graded-index OM1 multimode fiber using mode group division multiplexing," Opt. Exp. **24**, 18605–28594 (2016).
[23] R. S. Luís *et al.*, "Demonstration of a spatial super channel switching SDM network node on a field deployed 15-mode fiber network," ECOC'22, Th3B.5.
[24] G. Rademacher *et al.*, "Characterization of the first field-deployed 15-mode fiber cable for high density space-division multiplexing," ECOC'22, Th3C.1.